Geo-Marine Letters (2021) 41: 37
https://doi.org/10.1007/s00367-021-00710-x

ORIGINAL

Late Cretaceous to Miocene Paleoclimatic changes in the Indian Ocean: insights from the deepwater Mannar Basin, Sri Lanka

Amila Sandaruwan Ratnayake[1]

Received: 20 November 2020 / Accepted: 22 June 2021 / Published online: 21 July 2021

Abstract

The geology of Sri Lanka captures one of the longest and most complete records of Jurassic to Miocene tectonic evolutions from the mid-latitudes of the southern hemisphere to the equatorial northern hemisphere. Sedimentary basins in Sri Lanka provide a natural laboratory with which to reconstruct paleoclimate during the island's northward voyage from Gondwana to Asia. Here, drill core cuttings were obtained from the Barracuda hydrocarbon exploration well in the offshore Mannar Basin, Sri Lanka. CHNS elemental analysis, gas chromatography-mass spectrometry, and stable C and N isotopic analyses were performed. The results suggest the deposition of organic carbon depleted (average total organic carbon (TOC) = 0.97%) sediments under the arid climate of the Early Campanian. Separation of the Laxmi Ridge-Seychelles and Seychelles from the Indian plate and sea-level regression may have enhanced the deposition of organic carbon–rich (average TOC = 1.34%) and terrestrial organic matter (OM)–rich (average C/N ratio = 20.36) sediments during the Late Campanian to Late Maastrichtian. $CaCO_3$-rich (average = 32.5%) Upper Cretaceous sediments then show a period of high productivity under a warm climate. The Deccan-Reunion basalt likely acted as a major contributor to the mass extinction of coccolithophores/foraminifera at the Late Maastrichtian followed by a reduction of $CaCO_3$ and organic carbon content. The Early-Late Paleocene was characterized by the deposition of algal-derived OM with a terrestrial contribution (average C/N ratio = 15.75) under oxic depositional conditions (average C/S ratio = 16.21). However, the depositional environment changed drastically to one of oxygen-poor marine conditions (average C/S ratio = 6.83) during the Late Paleocene to the Early Oligocene due to weak oceanic circulation under a greenhouse climate. In contrast, the deposition of $CaCO_3$-rich sediments since the Late Paleocene (average = 40.2%) is linked to the movement of the Indian plate into northern, warmer tropical latitudes. The Middle Oligocene to Miocene sedimentary succession was characterized by terrestrial OM-rich (average TOC = 2.51% and C/N = 23.45) sediments. The Middle-Upper Miocene sedimentary succession contains lamination and back carbon (charcoal fragments) suggesting the development of the present-day South Asian monsoon system. This record from Sri Lanka provides important new insights into Jurassic-Miocene geological and climatic evolution in this tropical part of the world for the first time.

Introduction

Paleoceanic basins are excellent depositories of deep-time biological and geological records, and geological columns from these basins can yield important information for predicting biogeochemical processes and paleoclimate in Earth history (Pearson and Palmer 2000; Zachos et al. 2001; Hong et al. 2020). In particular, proxy records relating to the production, accumulation, and preservation of sedimentary organic matter (OM) responds in a very sensitive way to past palaeolatitudinal (tectonic), climatic, and oceanographic changes. The Cretaceous to Neogene period was a time of known fluctuations in greenhouse gas concentration, warm global temperature episodes, sea-level highstands, and stagnate oceanic circulation (e.g., Arthur et al. 1985; Raymo and Ruddiman 1992; Pearson and Palmer 2000; Zachos et al. 2001; Hong et al. 2020; Yang et al. 2020). These fluctuations are documented by stratigraphic and sedimentological features (Davies et al. 1995; Lu et al. 2019), paleontological and palynological data (Kaiho et al. 1999; Gupta and Kumar 2019), petrography and geochemistry (Dypvik et al. 2011; Teng et al. 2019), and isotopic geochemistry (Bains et al. 1999; Pälike et al. 2006; Hong et al. 2020). It is widely accepted that the tectonic evolution of Asia has played a

✉ Amila Sandaruwan Ratnayake
as_ratnayake@uwu.ac.lk

[1] Department of Applied Earth Sciences, Faculty of Applied Sciences, Uva Wellassa University, Passara Road, Badulla 90000, Sri Lanka

crucial role in many of these Earth systems phenomena over this critical period in the Earth's history.

The present tectonic configuration of Asia has evolved since the breakup of the Gondwana supercontinent during the middle Mesozoic. The offshore sedimentary basins of the Indian plate record a prolonged period of isolation before the subduction of this plate with the Eurasian (Asian) plate (Molnar and Tapponnier 1975; Ali and Aitchison 2008; Chakraborty et al. 2019). Therefore, the Indian Ocean is an ideal location for gaining a better understanding of regional and global environmental and climatic changes over geological time. However, it is poorly sampled compared to the other regions. Furthermore, geochemical studies have rarely been applied to develop continuous and long-term records from Cretaceous to Neogene sediments in the Indian Ocean.

The Mannar Basin is the largest peri-cratonic paleoceanic sedimentary basin in the Sri Lankan jurisdiction of the Indian Ocean (Ratnayake et al. 2014). Geochemical studies in the Mannar Basin (Fig. 1) have much promise for helping us to understand the relationships between carbon cycling and regional and/or global paleoclimatic changes in a portion of the Indian Ocean that has often been overlooked. In this study, the author examines the long-term factors controlling organic matter burial in the Mannar Basin. Variations in organic geochemical proxies (i.e., organic matter concentration and types and depositional environments) show how sedimentary records have responded to global and regional paleoclimatic changes, such as taxonomic diversification of calcareous microorganisms during the Late Cretaceous, K-Pg mass extinction, Deccan volcanism, the tectonic movement of the Indian plate, the Eocene–Oligocene climatic transition, and Cenozoic global cooling.

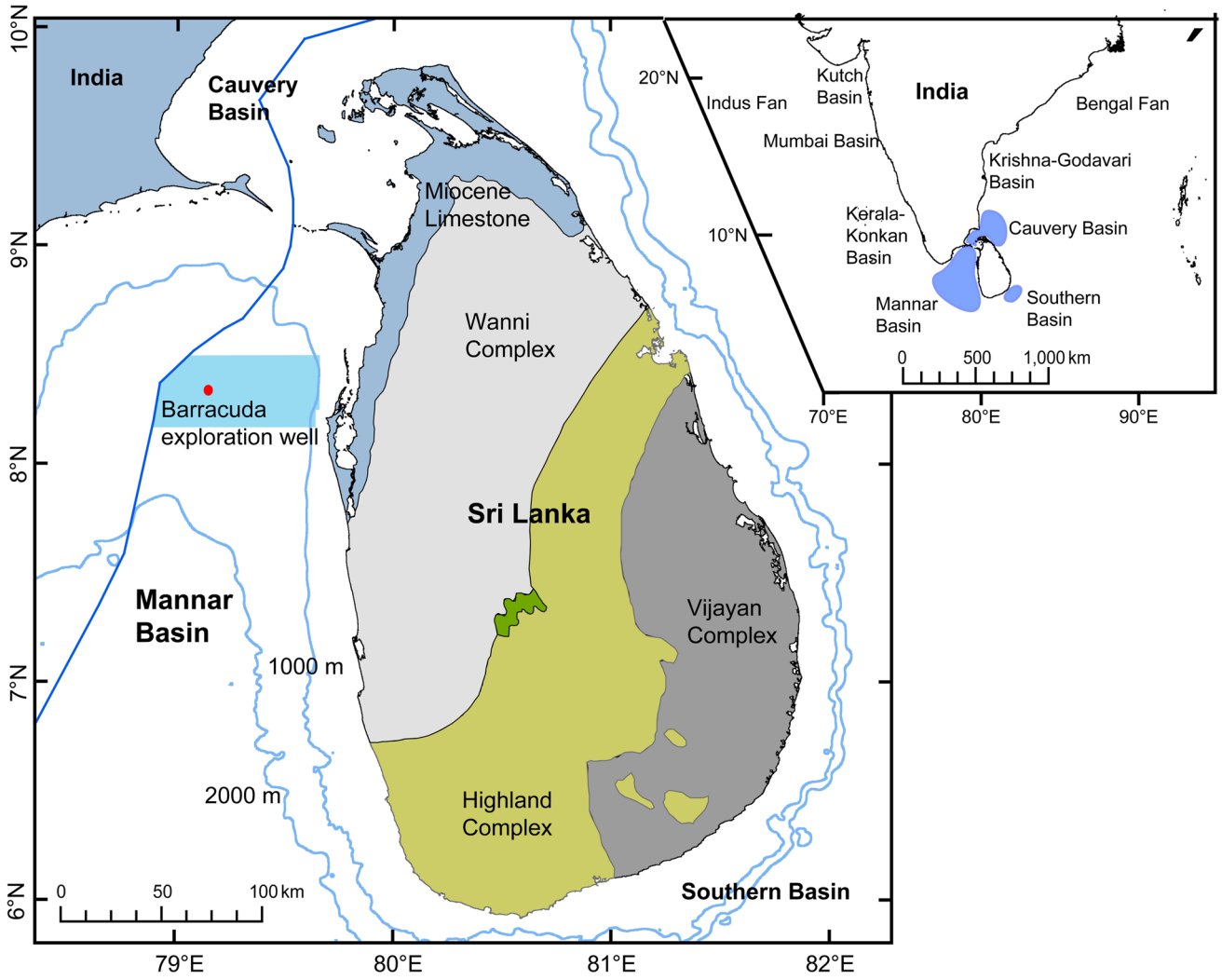

Fig. 1 Generalized map showing major geological units and offshore sedimentary basins in Sri Lanka. The inserted regional map shows the surrounding offshore sedimentary basins in the Bengal Fan and Indus Fan

Geological background

The Mannar Basin is situated in the southern part of the Indian subcontinent between the eastern portion of south India and western coast of Sri Lanka (Fig. 1). The basin contains a relatively thick succession of sediments spanning from the Late Jurassic to the Holocene (Ratnayake et al. 2014; Ratnayake and Sampei 2015; Kularathna et al. 2020). The sediments are underlain by Precambrian high-grade metamorphic rocks of amphibolite to granulite facies (Cooray 1984). The observed geological procession has its counterparts in geological outcrops in parts of south India and Sri Lanka such as the Achankovil Terrain in south India/Wanni Complex in Sri Lanka and the Thiruvananthapuram Terrain in south India/Highland Complex in Sri Lanka (e.g. Cooray 1984; Dissanayake and Chandrajith 1999; Bandara et al. 2020). Gravitational and magnetic anomalies observed in the southernmost part of the Mannar Basin indicate the presence of a highly attenuated and intruded continental to transitional crust as a lateral propagating tip of the seafloor spreading ridge (Sreejith et al. 2008).

The separation of East and West Gondwanaland resulted in the creation of the Indian Ocean between Greater India and East Antarctica during the Middle Jurassic (McKenzie and Sclater 1971; Norton and Sclater 1979; Chakraborty et al. 2019). The identified regional magnetic and gravitational anomalies show the tectonic evolutionary history of the study area (Rotstein et al. 2001; Desa et al. 2006; Nair and Pandey 2018; Lasitha et al. 2019). A rifting of India/Sri Lanka from East Antarctica (ca. 130 Ma; Ramana et al. 2001; Gaina et al. 2007; Chakraborty et al. 2019; Kapawar and Mamilla 2020) was followed by the opening of the Mannar Basin. This basin developed as a failed rift basin according to the regional tectonic framework. The Indian plate was subjected to several volcanic eruptions due to detachments of Madagascar (~ 90 Ma), Seychelles-Laxmi Ridge (~ 70 Ma), and Seychelles (~ 65 Ma) during the northward voyage (Storey et al. 1995; Subrahmanyam and Chand 2006; Nair and Pandey 2018). The collision of the Indian and Eurasian plates occurred in the Early Eocene (~ 50 Ma) and ultimately led to the build-up of the Himalaya and Tibetan Plateau (Le Fort 1975; Molnar and Tapponnier 1975; Chung et al. 1998; Chakraborty et al. 2019). After that, oceanic basins in the Indian plates closed at ~ 25 Ma with the completion of the India-Eurasian collision (Qin et al. 2019; Kapawar and Mamilla 2020). Consequently, the Mannar Basin gradually subsided since its rifting, leading to the deposition of marine and terrestrial sedimentary OM over ca. 167 million years from the Jurassic to Recent in age.

Materials and methods

Materials

The ` (PRDS) of Sri Lanka undertook an initial stage of offshore hydrocarbon exploration in the deepwater Mannar Basin using the *Chikyu* drillship. The 260 drill core cuttings were obtained at 10-m intervals from the Barracuda exploration well (coordinates: 08° 20′ 34.46″ N, 79° 09′ 39.38″ E in Fig. 1). The sampling depth ranges from 2139 to 4741 m, and the present water depth of the sampling site is 1509.0 m. All cutting samples were washed extensively to remove contaminated artificial oil-based drilling mud. Manual stirring and ultrasonic vibration methods were used following the addition of dichloromethane and methanol (9:1 v/v) solvent mixture. Ratnayake and Sampei (2019) provide a detailed methodology for the cleaning of cutting samples.

Methods

CHNS elemental analysis

Total carbon (TC), total organic carbon (TOC), total nitrogen (TN), and total sulfur (TS) percentages were determined with a FISONS Carlo Erba EA 1180 elemental analyzer using combustion method, at a combustion temperature of 1000 °C (the American Society for Testing and Materials (ASTM) method D5373). Total carbon content was first determined without HCl acidification for 260 samples. Samples were ground into a fine powder before analysis. About 10 mg of each sample was placed into tin capsules, which were crimp-sealed before analysis. Total organic carbon content was determined in a separate run for the same set of samples ($n = 260$), using powdered samples about 10 mg in weight. Accurately weighed samples were placed in a silver film. After that, a few drops of 1 M HCl were added to remove inorganic carbon and then dried at 110 °C for 45 min. The dried samples were sealed and placed into tin capsules, which were again sealed. The BBOT [2,5-bis(5-tert-butyl-2-benzoxazolyl)thiophene] standard was placed in a tin film. Regression analysis using this standard was used for quantitative analysis. All of the elemental percentages were calculated on a dry weight basis. Carbonate carbon percentages were calculated based on the difference between TC and TOC content. Carbonate carbon values were used to calculate $CaCO_3$ (%) in the samples.

GC–MS analysis

Sedimentary OM (bitumen, $n = 27$) was extracted using the Soxhlet apparatus with dichloromethane:methanol 9:1 v/v solution for 72 h. Elemental sulfur was removed using

activated copper granules. The less soluble portions present after extraction (inner cutting samples) were ground into a fine powder. The inner cutting samples were again extracted using the Soxhlet apparatus, refluxing using a dichloromethane:methanol 9:1 v/v solution for 72 h. Elemental sulfur was again removed using activated copper granules. Extracted OMs were separated into aliphatic and aromatic fractions utilizing thin layer chromatography (silica gel 60 PF_{254} containing gypsum) using hexane as a mobile phase under room temperature. Aliphatic and aromatic hydrocarbons were identified from the rest of the geolipids using UV light and were separated after washing with hexane.

Aliphatic and aromatic hydrocarbons were subsequently analyzed by gas chromatography (GC) and a mass spectrometer (MS; Shimadzu GCMS-QP 2010) system. The GC system (Shimadzu 2010) is equipped with a 30-m fused silica capillary column (DB 5MS, 0.25 mm film thickness) and used helium as a carrier gas. The GC oven temperature was programmed to increase from 50 to 300 °C at the rate of 8 °C/min before being held at 300 °C for 30 min. The MS was scanned every 0.5 s from *m/z* 50 to 850, and all spectral data were automatically stored in the computer system. The ionization energy of the MS was set at 70 eV. The organic compounds were recognized by comparison of retention times and mass spectra with published data and reference standards.

$\delta^{13}C$ and $\delta^{15}N$ isotope analysis

Twenty-seven powdered samples were combusted at 1800 °C, with the evolved gases being carried by helium (90 mL/min), and passed through catalysts, to convert CO into CO_2. Elemental copper in the reduction column reduces NO and NO_2 to elemental N_2. Nitrogen and carbon dioxide gasses were separated by gas chromatography (GC) column and analyzed for $\delta^{13}C$ and $\delta^{15}N$ using a Thermo Fisher Scientific Delta V Advantage Isotope Ratio Mass Spectrometer (IRMS) coupled with a Carlo Erba NC 2500 elemental analyzer at Illinois State Geological Survey, USA.

Ammonium sulfate standards and an internally calibrated amino acid standard were analyzed as nitrogen standards (see Appendix A for laboratory standards and 5-point calibration curve). Samples were calibrated and reported as $\delta^{15}N$ vs. air. Atropine, IAEA-600 caffeine, USGS-40, and amino acid L-serine were analyzed as carbon standards (see Appendix A for laboratory standards and 4-point calibration curve). Samples were calibrated and reported relative to Vienna Pee Dee Belemnite (VPDB). The results show the precision of the $\delta^{15}N$ measurements to be better than $\pm 0.22‰$ and that of the $\delta^{13}C$ analysis to be better than $\pm 0.11‰$.

Stratigraphy and age model

Biostratigraphic charts of the Barracuda well were obtained from the Petroleum Resources Development Secretariat (PRDS) of Sri Lanka to tabulate the age of the sedimentary column. These unpublished data were generated using seismic data, well logs, and biostratigraphic studies of micropalaeontological, nannopalaeontological, and palynological assemblages. Kularathna et al. (2020) published the generalized stratigraphic column of the Barracuda well, providing a crucial reference for this study.

Results and discussion

Variations of carbonate deposition

Figure 2 shows the variations in carbonate accumulations through the Barracuda well record in the Mannar Basin (see Appendix B for primary data). The accumulation and preservation of carbonate particles in marine sediments is controlled by several factors, as discussed below. In this study, carbonate-rich strata were recorded from the Early Campanian to Late Maastrichtian stages (from 4270 to 4741 m, $CaCO_3 = 32.50\% \pm 9.42$ in Fig. 2c). Late Cretaceous carbonate accumulation may indicate the effects of the taxonomic diversification of calcareous nannofossils and planktonic foraminifera (Boss and Wilkinson 1991; Huber and Watkins 1992; Ridgwell and Zeebe 2005), as well as the precipitation of $CaCO_3$ under high atmospheric CO_2 (ca. 2500 ppm) level (Ridgwell and Zeebe 2005; Kent and Muttoni 2008). The weathering of silicate and carbonate rocks also plays a major role in the burial of terrestrial carbonate flux under warmer and more humid climates (Berner et al. 1983; Arthur et al. 1985; Teng et al. 2019). Therefore, the reduction of carbonate deposition in the Upper Maastrichtian volcanogenic sediments can be recognized as being indicative of major environmental changes (i.e., alteration of oceanic chemistry and/or the open-ocean ecosystem) in the Indian Ocean (Fig. 2c).

The K-Pg mass extinction event was characterized by a sharp reduction in carbonate productivity for several hundred thousand years (e.g., Caldeira and Rampino 1993; Gertsch et al. 2011). This period is globally characterized as involving the extinction of about 85% of planktonic foraminifera and calcareous nannofossils in the marine ecosystem (Zachos et al. 1989; D'Hondt et al. 1998). Therefore, the reduction of carbonate accumulation, along with TOC (Fig. 2), is likely associated with a collapse of aquatic productivity (super-stress conditions) across the K-Pg boundary in the Mannar Basin. The published records in the Indian Ocean also indicate the enhancement of carbonate dissolution due to acidification following Deccan volcanism. It has also been considered to have

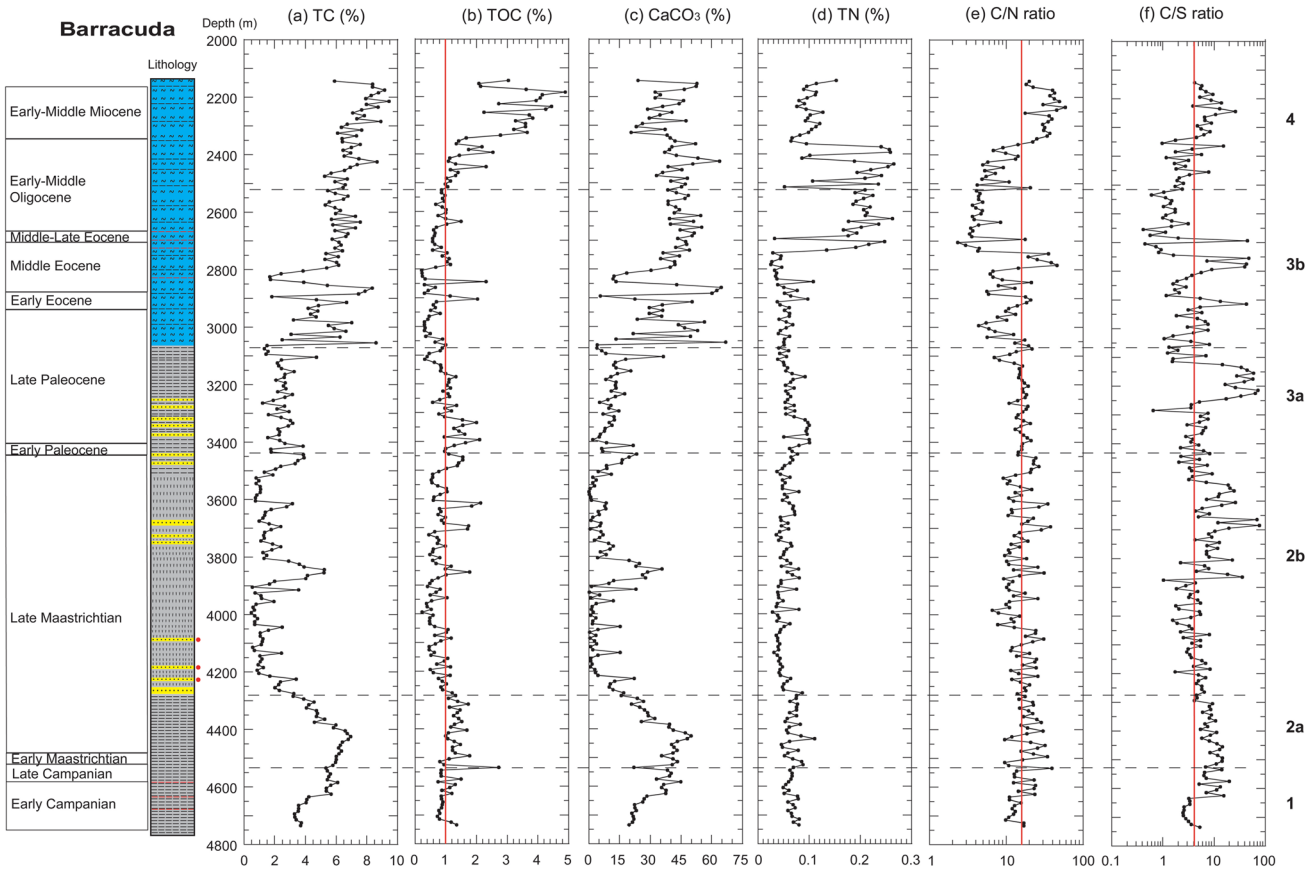

Fig. 2 Vertical distributions of **a** TC (%), **b** TOC (%), **c** $CaCO_3$ (%), **d** TN (%), **e** C/N ratio, and **f** C/S ratio of the Barracuda well record from the Mannar Basin

catalyzed biotic stress (reduction in diversity) and/or the mass extinction of planktonic foraminifera and calcareous nannofossils in the Indian Ocean during the Late Maastrichtian based on records from the Ocean Drilling Project (ODP) Leg 121, Ninetyeast Ridge Deep Sea Drilling Project (DSDP) Sites 216 and 217, Wharton Basin Site 212, and Krishna-Godavari Basin (Rea et al. 1990; Keller 2003; Keller et al. 2008; Tantawy et al. 2009).

Carbonate deposition is low in the Lower Paleocene to Upper Paleocene sediments of the Barracuda well (average $CaCO_3 = 11.13\% \pm 6.14$). However, carbonate deposition drastically increased from the Late Paleocene. The development of a $CaCO_3$ platform from the Late Paleocene (close to the Paleocene-Eocene boundary) is primarily correlated with the transition from an arid climate into a warm and humid tropical climate following the movement of the Indian plate (including Sri Lanka) northward into warmer, equatorial latitudes. According to the literature, the weathering of Himalayan rocks has been generally identified to be the main cause behind increments of carbonate flux during the Late Cenozoic in the Bay of Bengal and Indus Fan sediments (France-Lanord and Derry 1997; Métivier et al. 1999; Zachos et al. 2001; Parmar et al. 2020).

Carbonate accumulation was enhanced in the Barracuda well (average $CaCO_3 = 40.20\% \pm 12.14$) since the Late Paleocene. Consequently, the uplifted Precambrian rocks in Sri Lanka and the Eastern Ghats, India (e.g., Cooray 1984; Bose et al. 2020) have been influenced by the carbonate burial in the Mannar Basin due to combined rapid physical denudation with chemical weathering within a tropical climate. This idea is supported by an observed enhancement of greenhouse conditions and monsoon-like rainfall patterns in Asia during the Eocene (Licht et al. 2014; Teng et al. 2019). In addition, based on basin modeling interpretations (Ratnayake et al. 2014), carbonate burial was likely enhanced by open marine and deepwater conditions (e.g., Adatte et al. 2002; Gertsch et al. 2011) following tectonic subsidence in the Mannar Basin from the Eocene (average subsidence rate = 16 m/Ma) to Miocene (average = 19 m/Ma).

Variations of organic matter delivery

The average TOC content in the Lower–Upper Campanian sediments (from 4540 to 4741 m) of the Barracuda well is 0.97% ± 0.23 (Fig. 2b). The Upper Campanian to Upper Maastrichtian sediments of the Barracuda sequence are rich in OM (from 4270 to 4540 m, average TOC = 1.34% ± 0.36 in Fig. 2b). Late Cretaceous organic carbon deposition has an apparent relationship with carbonate deposition (Fig. 2).

TOC values are slightly decreased in the Lower–Upper Paleocene sediments of the Barracuda well (from 3060 to 3440 m, average = 1.07% ± 0.39 in Figs. 2b). Although carbonate accumulation is considerably enhanced in the sediments from the Upper Paleocene to the Lower-Middle Oligocene, organic carbon accumulation is relatively low in this portion of Barracuda well sequence (2520–3060 m, average = 0.74% ± 0.41). The reduction of organic carbon accumulation in these strata is likely driven by limited nutrient mixing (low oceanic primary productivity) as a result of weak paleoceanic currents during the Eocene to Early Oligocene in response to low global latitudinal temperature gradients between poles and topics under the greenhouse climate (Davies et al. 1995; Licht et al. 2014). However, TOC content gradually increased from the Middle Oligocene (Fig. 2b).

The analysis of sedimentary facies revealed that OM-rich Middle Oligocene to Miocene beds consist of black carbon and laminations (Ratnayake et al. 2014), suggesting seasonal changes in the watershed. The Middle Oligocene to Miocene (ca. 380-m thick) sedimentary sequence of the Barracuda well indicates a higher amount of OM preservation (average TOC = 2.51% ± 1.20). This observation was linked with records of major sea-level regression (marked by erosional unconformity) and continental sedimentation along rift-passive margin sedimentary basins in the Indian subcontinent since the Oligocene (e.g., Adatte et al. 2002; Nair and Pandey 2018; Chakraborty et al. 2019). In this study, Middle Oligocene to Miocene OM-rich beds were deposited after the Eocene–Oligocene climatic transition ca. 34 Ma ago (Pearson and Palmer 2000; Pearson et al. 2009). It is possible that this event had a teleconnection with the formation of the Antarctic ice sheet and resulted in the drop of global sea level, as demonstrated by simulations and proxy analyses across the globe (e.g., Volk 1989; Raymo and Ruddiman 1992; Gaillardet and Galy 2008) that characterize the state of the Earth today.

Variations of organic matter type delivery

Bulk C/N ratios, biomarkers, and stable $\delta^{13}C$ isotope values have been widely applied to paleoclimatic records in order to identify OM sources and assess changes in the availability of nutrients (e.g., Meyers and Ishiwatari 1993; Sampei and Matsumoto 2001; Ratnayake and Sampei 2015; Gupta and Kumar 2019; Li et al. 2020). C/N ratios reveal that the Lower–Upper Campanian sediments consist of a mixture of terrestrial and algal-derived OM (average = 15.13 ± 4.68 in Fig. 2e). The *m/z* 57 mass chromatograms of the Lower–Upper Campanian sediments in the Barracuda document a nC_{19} dominant bimodal pattern with maxima at the nC_{22}/nC_{23} and nC_{31} peaks (Fig. 3a). The middle-chain length (nC_{23} and nC_{25}) *n*-alkane homologues can be recognized as sources of bog-forming aquatic vegetation in swamps (Ficken et al. 2000; Pancost et al. 2002; Bingham et al. 2010; Ratnayake and Sampei 2015). The abundance of the nC_{31} homologue also indicates the occurrence of grasses (graminoids) and shrub-type herbaceous vegetation in swamps (Zhou et al. 2005; Castañeda et al. 2009; Ratnayake et al. 2017). Therefore, the Lower–Upper Campanian sediments of the Barracuda well record a higher amount of terrestrial (average C_{20}-C_{26}/nC_{all} = 0.67 ± 0.08) carbon sources (Fig. 4).

The C/N ratios of organic carbon-rich Upper Campanian to Upper Maastrichtian sediments of the Barracuda (4270–4540 m, average = 20.36 ± 7.64) well indicate an accumulation of higher plant wax dominant sediments (Fig. 2e). Biomarker studies also indicate a higher amount of middle-chain (nC_{21} to nC_{25}) and long-chain (nC_{27} to nC_{31}) *n*-alkanes from vascular plant waxes (Fig. 3b). Similarly, Ratnayake et al. (2018) identified occurrences of oil and gas prone (type II-III) and gas prone (type III) kerogen, based on Rock–Eval pyrolysis data in the Lower Campanian to Upper Maastrichtian sediments of the Mannar Basin. Therefore, the increment of TOC and vascular plants OM in this sedimentary succession suggests the deposition of continental sediments in the Mannar Basin, likely as a result of sea-level regression in nearshore environments and tectonic changes (e.g., Huber and Watkins 1992; Adatte et al. 2002; Keller 2003, 2005; Gertsch et al. 2011; Clift 2020). The available literature suggests that sea-level regression was generally associated with widespread continental erosion during the Late Maastrichtian (e.g., Abramovich et al. 2002; Adatte et al. 2002; Keller 2004). Moreover, the rapid evolution and expansion of angiosperms since the Middle Cretaceous (Hickey and Doyle 1977) may have gradually increased the burial rate of terrestrial OM in coastal swamps. This idea is supported by high values in terrestrial biomarker proxies of $> nC_{26}/nC_{all}$ (average = 0.17 ± 0.04) and average-chain length (ACL, average = 26.47 ± 1.14) compared to the underling Campanian sedimentary sequence ($> nC_{26}/nC_{all}$ average = 0.14 ± 0.06 and ACL average = 25.80 ± 0.73) in the Barracuda well (Fig. 4). The volcanogenic sediments of the Barracuda well also indicate the deposition of terrestrial OM (Figs. 2e and 3c).

The Paleocene sequence (3060–3440 m, average C/N = 15.75 ± 3.19 in Fig. 2e) contains mixtures of terrestrial and algal-derived OM. Similarly, the Upper Paleocene

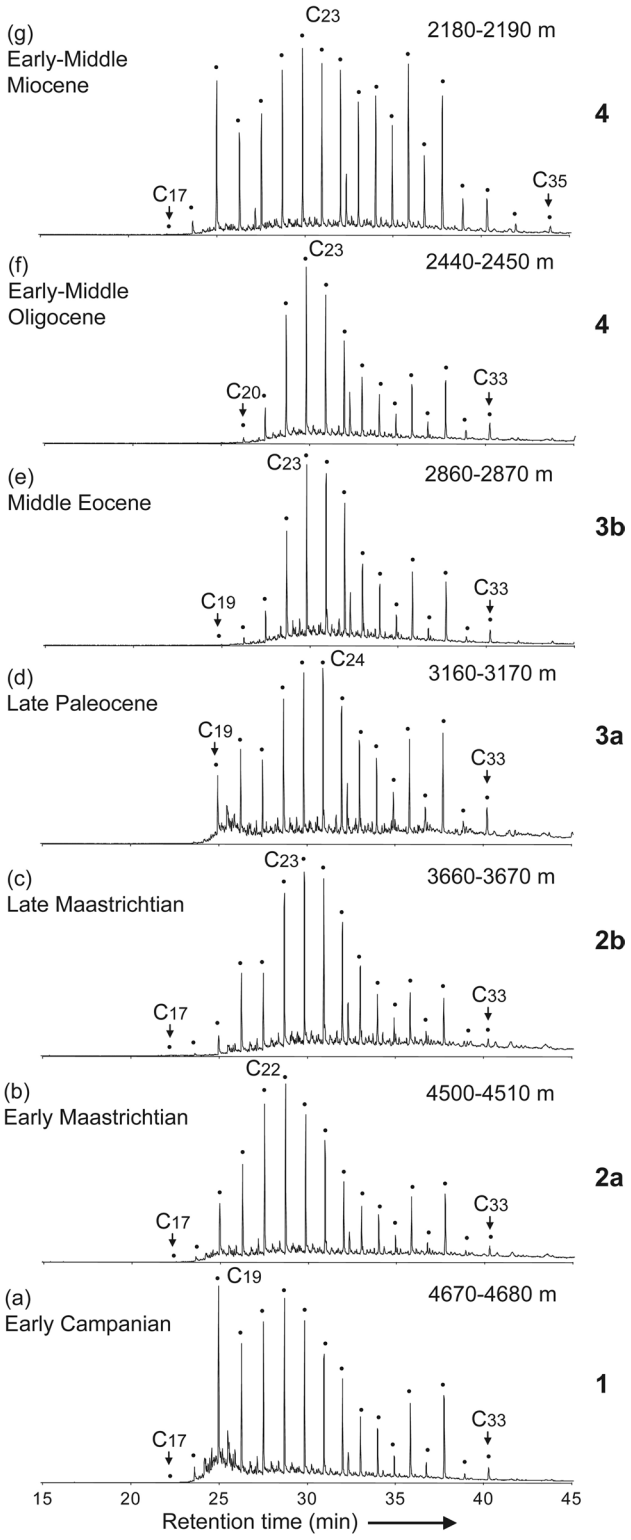

Fig. 3 Mass chromatograms ($m/z = 57$) showing the distribution of *n*-alkanes in the Barracuda well record

sediments of the Barracuda well show an intensification in the frequency of middle-chain length nC_{23} *n*-alkanes with higher molecular weight ($> nC_{26}$) *n*-alkanes (Fig. 3d). The Upper Paleocene to the Lower-Middle Oligocene argillaceous marl/marlstone sediments indicate algal-derived OM with some terrestrial contributions (2520–3060 m, average = 13.78 ± 10.00 in Fig. 2e). The *n*-alkane distributions in this sedimentary succession also indicate an enhancement of higher plant wax ($> nC_{20}$ in Fig. 3e) from terrestrial sediments (C_{20}-C_{26}/nC_{all} average = 0.75 ± 0.15, $> nC_{26}/nC_{all}$ average = 0.25 ± 0.15 and ACL average = 26.00 ± 1.28 in Fig. 4).

Terrestrial OM distribution increased from the Middle Oligocene to Lower Miocene portions of the sedimentary succession from the Barracuda well (2139–2520 m, average = 23.45 ± 15.02 in Fig. 2e). The *n*-alkane mass chromatogram indicates higher plant wax ($> nC_{20}$) dominant sediments during the Early-Middle Oligocene (Fig. 3f), followed by continental erosion that has been recorded in surrounding sedimentary basins in the Indian subcontinent (e.g., Nair and Pandey 2018; Chakraborty et al. 2019; Parmar et al. 2020). In addition, the available Rock–Eval data suggested that OMs are primarily of terrigenous (type III/II) origin (Ratnayake et al. 2018). Furthermore, the Lower-Middle Miocene sediments in the Barracuda well consist of fine-grained black carbon/charcoal fragments (Ratnayake et al. 2014) with a higher amount of long-chain *n*-alkanes ($> nC_{26}$) (Fig. 3g). This suggests the deposition of long-distance transported OM. Consequently, these changes suggest the strengthening/development of the South Asian monsoon from the Early-Middle Miocene, as has been demonstrated elsewhere (e.g., Quade et al. 1989; Dettman et al. 2001; Gupta et al. 2004; Clift 2020).

In this study, a considerable number of samples recorded abnormally low C/N ratios (< 4) due to the absorption of inorganic nitrogen (NH_4^+) in fine-grained sediments (Müller 1977; Sampei and Matsumoto 2001). These low C/N ratios suggest that inorganic nitrogen absorption was prominently recorded in the Middle Eocene to Lower Oligocene sediments of the Barracuda well (Fig. 2e). In addition, TN values drastically increased, without TOC increments, in the Middle Eocene to Lower Oligocene sediments of the Barracuda well (Fig. 2). These episodes signify the enrichment of inorganic nitrogen rather than nutrient accumulations over geological time. In this study, samples with abnormally low C/N values (< 4) were removed from calculations of the average and standard deviations for each stratum.

Stable carbon ($\delta^{13}C$) isotopic values are thus likely more reliable for reconstructing past sources of OMs under different depositional conditions in this record. Terrestrial C_3 and C_4 plants show an average $\delta^{13}C$ value of ca. − 28 ‰ and ca. − 14 ‰, respectively (Bender 1971; Chikaraishi and Naraoka 2005; Lamb et al. 2006; Gupta and Kumar 2019; Hong et al. 2020). The $\delta^{13}C$ isotopic composition of plant

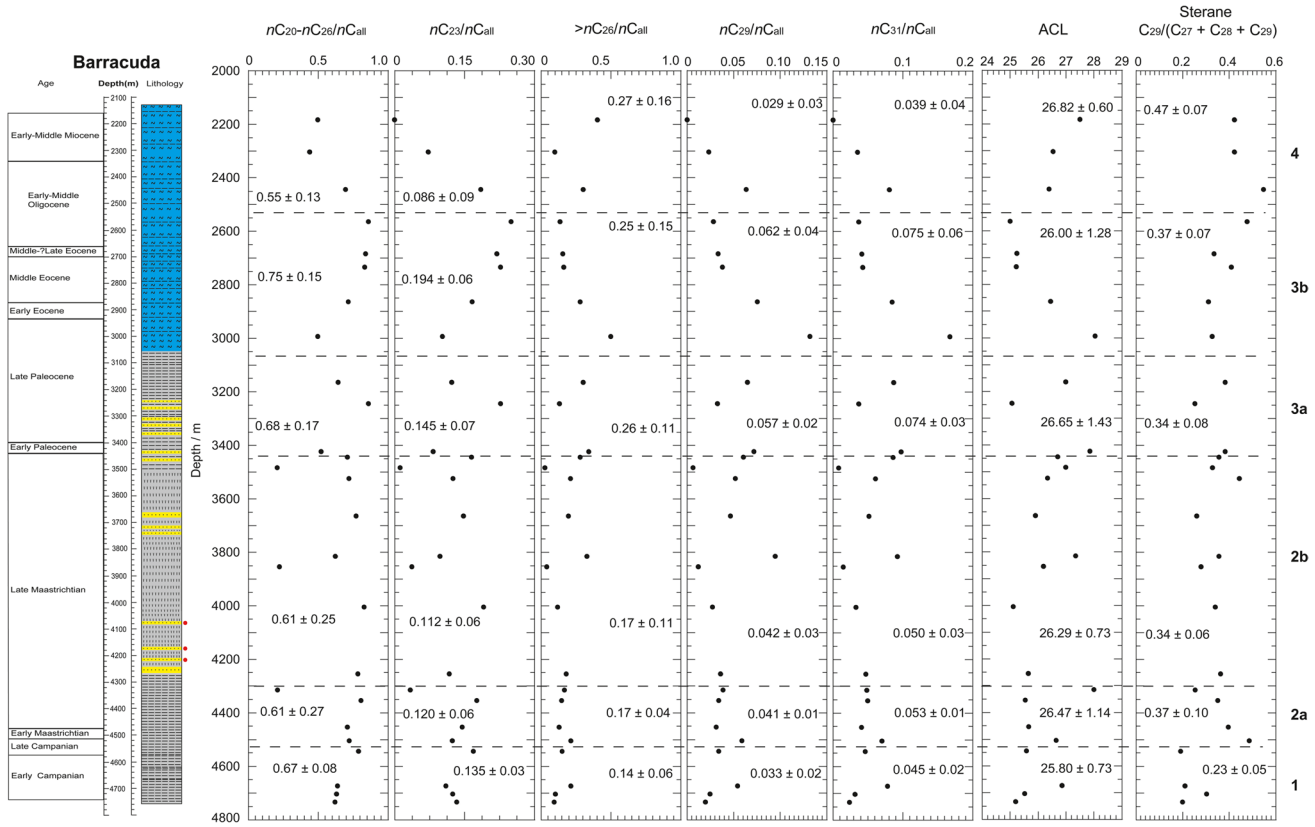

Fig. 4 Biomarker results from the Barracuda well record

biomass is thus primarily a function of the photosynthetic pathway (Bender 1971), with no influence of grain size effects. Overall, based on these data, it is clear that core sediments in the Mannar Basin derive mainly from C_3 plant dominant terrestrial sources (Fig. 5 and see Appendix A for primary data).

Depositional environments

TOC to TS relationship (C/S ratio) is an indicator of depositional processes such as sulfate reduction, Fe-S cycling, paleosalinity, and early diagenesis (e.g., Berner 1982, 1984; Meyers and Ishiwatari 1993; Sampei et al. 1997a; Teng et al. 2019). C/S ratios reveal that the lowermost Campanian sediments show oxygen-poor conditions (average = 6.38 ± 4.93 in Fig. 2f). C/S ratios indicative of organic carbon-rich conditions in the Upper Campanian to Upper Maastrichtian sediments (4270–4540 m, average = 9.15 ± 3.22) suggest a comparatively less reducing environment (Fig. 2f). The relatively high C/S ratios compared to the bottom of the sedimentary succession may indicate a lower activity of sulfate-reducing bacteria in terrestrial OM-rich sediments (e.g., Berner 1984; Gong and Hollander 1997; Sampei et al. 1997a).

C/S values for the Lower–Upper Paleocene portion of the sequence, ranging from ca. 10 to less than 100, show wide and cyclic fluctuations. Furthermore, wide variations in C/S ratios of the Barracuda well record indicate weaker reducing characteristics in sand dominant turbidities (3060–3440 m, average 16.21 ± 20.14 in Fig. 2f).

C/S ratios are low from the Upper Paleocene to the Lower-Middle Oligocene portion of the record (2520–3060 m, average = 6.83 ± 12.24 in Fig. 2f). This implies an oxygen-depleted environment. Similarly, alternating dark and light color laminations in this sedimentary succession signify cyclic changes in supplies of sediments under anoxic/reducing conditions (Gong and Hollander 1997; Meyers 2003; Valdés et al. 2004; Lokho et al. 2020). This interpretation is consistent with observed monsoon rainfall patterns in Asia (Licht et al. 2014; Teng et al. 2019) and stratified and weak ocean circulation in the Indian Ocean during the Eocene (Davies et al. 1995). By contrast, a few outliers (range from 39.88 to 47.97, $n = 5$) increase the average C/S ratio of the Barracuda well during the Upper Paleocene to the Lower-Middle Oligocene period (Fig. 2f). This can be interpreted as an influence of strong short-term and deepwater oceanic currents under open marine conditions. C/S ratios (average = 5.98 ± 4.96) of the Middle Oligocene to Lower

Miocene sediments of the Barracuda well can be explained as reflecting deposition of less reducing terrestrial OM-rich sediments within a deepwater marine setting.

Paleoenvironment and paleoclimate

Four major paleoclimatic chronozones were recognized in the Mannar Basin, based on sedimentary facies, OM quantity/type, and depositional changes (Fig. 6). The lowermost period (chronozone 1: Early Campanian) consists of organic carbon-depleted (average TOC = 0.97%) sediments. In this period, algae-dominant OM was deposited with terrestrial OM (average C/N ratio = 15.13) under oxygen-poor depositional environments (average C/S ratios of Barracuda = 6.38). The Mannar Basin was situated in the arid climate belt during the Early Campanian (Lees 2002; Scotese et al. 2011). Similarly, ca. 720 mm/year precipitation is estimated for eastern part of the Indian subcontinent at this time, according to the Fast Ocean-Atmospheric Model (Chatterjee et al. 2013).

Chronozone 2a in Fig. 6 (Late Campanian to Late Maastrichtian) is composed of organic carbon-rich sediments (average TOC = 1.34%). These terrestrial OM-rich (average C/N ratio = 20.36) sediments were deposited under less reducing conditions (average C/S ratio = 9.15). Several smaller continental blocks such as the Laxmi Ridge-Seychelles (~ 70 Ma) and Seychelles (~ 65 Ma) were separated from the Indian plate during the Late Maastrichtian (Storey et al. 1995; Subrahmanyam and Chand 2006; Calvès et al. 2011; Rao and Singh 2020). Tectonic forcing and a drop of sea level (Huber and Watkins 1992; Gombos et al. 1995; Keller 2003, 2005; Clift 2020) were followed by the

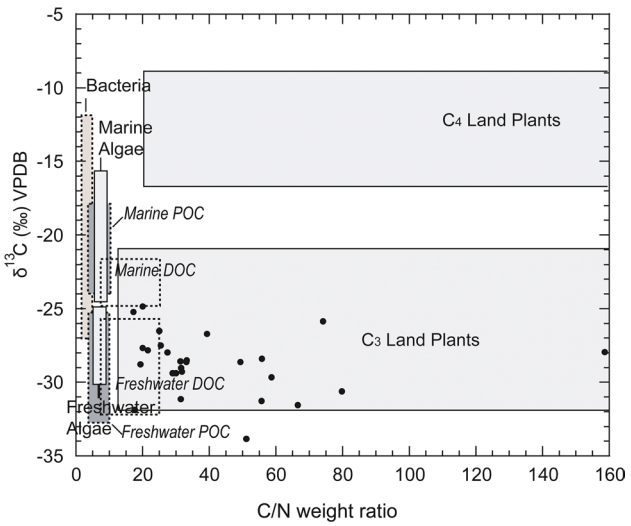

Fig. 5 Relationship between isotopic $\delta^{13}C$ and elemental C/N ratio shows sources of organic matters (modified after Meyers 2003 and Lamb et al. 2006) (where POM, particulate organic matter and DOC, dissolved organic carbon)

deposition of terrestrial OM-rich sediments. Although the Mannar Basin was located in the arid to subtropical temperate climatic zone during the Late Campanian to Late Maastrichtian (Lees 2002; Scotese et al. 2011), a broadly warmer and wetter global climate than the present, with the exception of short-term global cooling events (Arthur et al. 1985; Adatte et al. 2002; Keller et al. 2015; Yang et al. 2020), may have influenced this process. In this period, the Indian plate became smaller and smaller in size and resided as an island continent in the southern hemisphere. Previous investigations, as well as the data recorded in this study, indicate that paleoceanic basins in the Indian plate were characterized by the deposition of thick carbonate sediments during the Late Cretaceous (e.g., Rao 2001; Chatterjee et al. 2013; Teng et al. 2019). The carbonate-rich pelagic sediments of this region are likely a product of the known evolutionary diversification of microorganisms and high partial pressure of atmospheric carbon dioxide (pCO_2) under warmer climatic conditions, during the Late Campanian to Late Maastrichtian (Kent and Muttoni 2008; Keller et al. 2015). Carbonate depletion at the K-Pg boundary indicates super-stress environmental conditions, including greenhouse warming, eutrophication, and acid rain over the Indian subcontinent (e.g., O'Keefe and Ahrens 1989; Sigurdsson et al. 1992; Gertsch et al. 2011). The super-stress environmental conditions are associated with Deccan volcanism and are marked by the extinction of an abundance of foraminifera in the Indian Ocean (e.g., Keller 2003, 2005; Keller et al. 2015).

Chronozone 2b subcategory is characterized by the deposition of volcanogenic sediments due to several episodes of Deccan-Reunion basalt volcanism at the top of the Late Maastrichtian (Fig. 6). Ratnayake et al. (in preparation) examined the provenance of the Upper Maastrichtian volcanogenic sediments in the Mannar Basin using whole-rock geochemistry. These unpublished data reveal that the Upper Maastrichtian mafic sources are linked to the Deccan basalt volcanisms, and a significant difference can be observed compared to the adjacent sedimentary strata. In contrast, this sedimentary succession indicates relatively high TOC values (average = 0.84%) under a high mud sedimentation rate of 49 m/Ma (Ratnayake et al. 2014). Previous investigations showed that high sedimentation rates (> ca. 40 m/Ma) decrease TOC content due to clastic dilution (e.g., Berner 1982; Ibach 1982; Sampei et al. 1997b; Li et al. 2020). Therefore, high TOC values of the Upper Maastrichtian volcanogenic sediments also suggest warmer climatic conditions and higher fertility (primary productivity), triggered by submarine igneous events and favorable preservation of OM.

Chronozone 3a in Fig. 6 (Early-Late Paleocene) records OM-poor to moderate sediments (average TOC = 1.07%). Published work suggest that low marine productivity had gradually recovered more than 3 Ma after the K-Pg mass extinction (D'Hondt et al. 1998), under the semiarid to arid

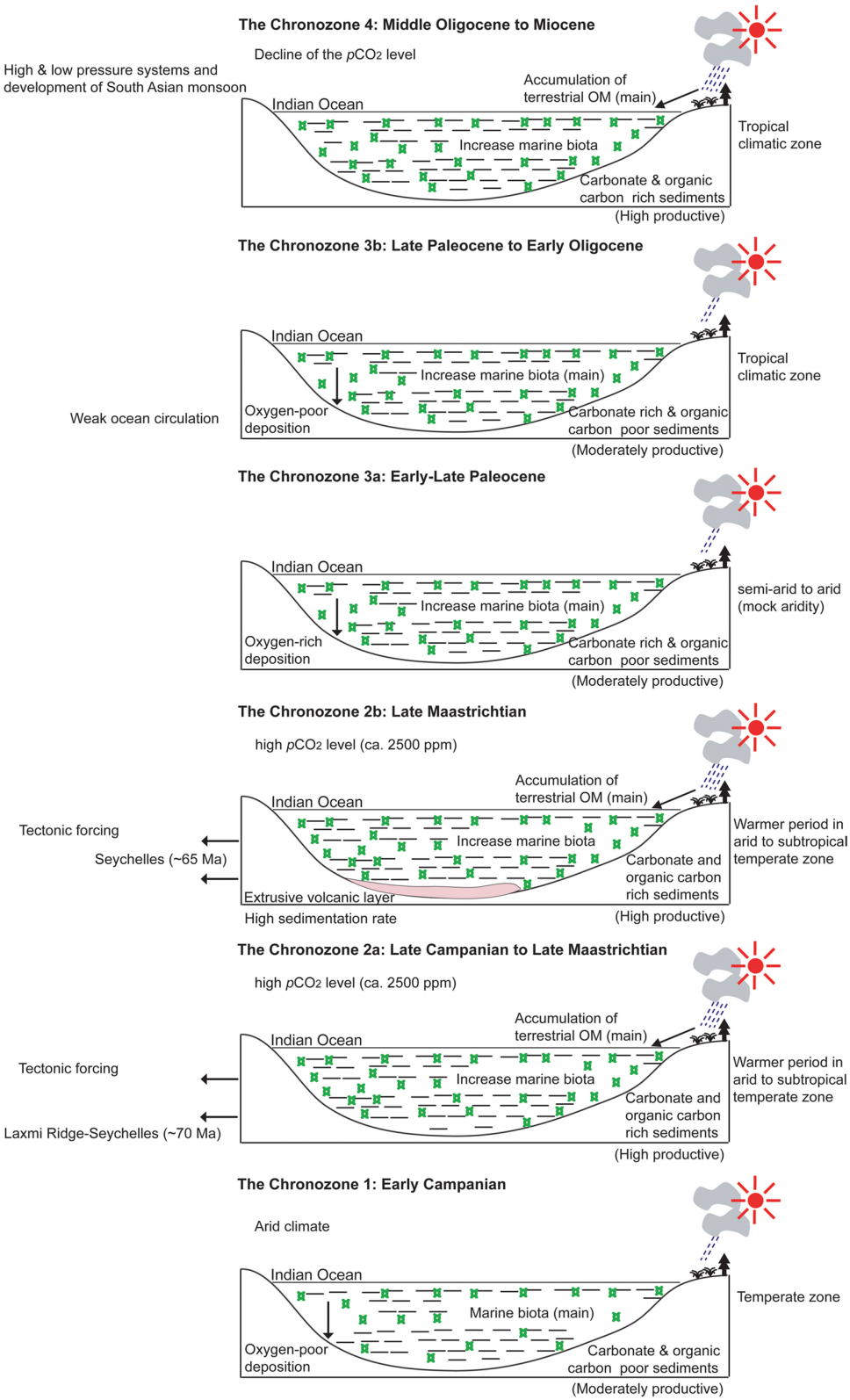

Fig. 6 Schematic of cross sections for the major paleoclimate chronozones identified in the Mannar Basin record

(mock aridity) climate of the Early Danian on the Indian subcontinent (e.g., Gertsch et al. 2011). In addition, this period is characterized by the deposition of algae-dominant OM with terrestrial sediments (average C/N ratio = 15.75) under oxic depositional conditions (average C/S ratio = 16.21). In contrast, the Late Paleocene was characterized by noticeably

higher concentrations of CO_2 (ca. 2000 ppm) and other greenhouse gases compared to the present day (Pearson and Palmer 2000; Zachos et al. 2001, 2008). For example, the Late Paleocene Thermal Maximum (LPTM) represented the warmest interval of the Cenozoic at the Paleocene/Eocene (ca. 55 Ma) boundary (Bains et al. 1999; Zachos et al. 2001, 2005; Lourens et al. 2005; Gupta and Kumar 2019). The Mannar Basin was characterized by the enhancement of carbonate-rich pelagic sediments (carbonate platform) near the Paleocene/Eocene boundary under a tropical (equatorial) humid climate.

In chronozone 3b, the Late Paleocene to the Early Oligocene, OM concentration (average TOC = 0.74%) and type (average C/N ratio = 13.78) remain almost constant (Fig. 6). However, in this sub-chronozone, the depositional environment changed to oxygen-poor marine conditions (average C/S ratio = 6.83), perhaps as a consequence of weak ocean circulation in the Indian Ocean under the greenhouse climate (Davies et al. 1995; Licht et al. 2014).

The Middle Oligocene to Miocene sedimentary succession of the Barracuda well represents chronozone 4 (Fig. 6). In this section, a higher amount of terrestrial debris (average C/N ratio = 23.45) was deposited within a marine depositional environment (average C/S ratio = 5.98). This sedimentary succession indicates the enhancement of organic burial (average TOC = 2.51%) after the Eocene–Oligocene climate transition (ca. 34 Ma), which is marked by the sharp decline of atmospheric CO_2 concentration due to the growth of the Antarctic ice sheets (Raymo and Ruddiman 1992; Pearson and Palmer 2000; Pälike et al. 2006; Tripati et al. 2009). The Indian subcontinent had achieved its present-day configuration by the Miocene. The subcontinental landmass thus provided a source of insolation in the lower atmosphere during the summer, which produced a strong low-pressure system over the region. The uplifted mountains act as a barrier and resulted in the development of South Asian monsoon precipitation which is continuous to the present (e.g., Quade et al. 1989; Dettman et al. 2001; Zhisheng et al. 2001; Gupta et al. 2004; Harris 2006; Clift 2020). Therefore, OM-rich beds, lamination, back carbon/fine-grained charcoal fragments, and the domination of mass chromatograms by long-chain *n*-alkanes ($> nC_{26}$) indicate the development of South Asian monsoon from the Middle to Late Miocene.

Conclusions

The Mannar Basin record provides the first geological and paleoclimatic proxy sequence spanning the Jurassic to the Miocene for Sri Lanka, a landmass that was at the center of tectonic change and rafting (e.g., the breakup of Gondwana), oceanic circulation evolution, and mass extinction events during this span of time. Calcareous nannofossils and planktonic foraminifera diversified during the Early Campanian to Late Maastrichtian under a warm climate. The diversity of microorganisms was then drastically reduced toward the K-Pg boundary under the influence of Deccan-Reunion volcanism in the Indian Ocean. Tectonic forcing and sea-level regression controlled the deposition of terrestrial OM and organic carbon-rich sediments during the Late Campanian to Late Maastrichtian. The development of a $CaCO_3$ platform around the Late Paleocene-Eocene boundary was linked to the influence of a tropical climate and continuous subsidence of the basin. The Eocene epoch was characterized by weak oceanic circulation in the Indian Ocean under the greenhouse climate. Finally, the drop in sea level after the formation of the Antarctic ice sheets is associated with the deposition of terrestrial OM-rich sediments since the Middle Oligocene and the development of the Indian Ocean monsoon system which characterizes the climate of the region to this day. It is hoped that the Mannar Basin record acts as an important reference for further research into the geological and climatic evolution of the equatorial latitudes of Asia across this important time frame in Earth's history.

Supplementary Information The online version contains supplementary material available at https://doi.org/10.1007/s00367-021-00710-x.

Acknowledgements The author would like to acknowledge the financial support for this study provided by Accelerating Higher Education Expansion and Development (AHEAD) Development Oriented Research (DOR) grant. The author also acknowledges the support of MEXT Scholarship (the Japanese Ministry of Education and Culture) for completing early-stage research publications linked to this project. Furthermore, I would like to greatly acknowledge Prof. Yoshikazu Sampei, Shimane University Japan, and Prof. Thomas Algeo, University of Cincinnati, USA, for valuable comments and suggestions. I would also like to thank Director General Saliya Wickramasuriya and Petroleum Geologist C.W. Kularathne of the Petroleum Resources Development Secretariat (PRDS) of Sri Lanka for providing the rock cuttings for this study. I thank Dr. Patrick Roberts, Max Planck Institute for the Science of Human History, Germany, for editorial suggestions, and Dr. Andrew Green, Editor-in-Chief, and anonymous reviewers for their help and critical reviews.

References

Abramovich S, Keller G, Adatte T, Stinnesbeck W, Hottinger L, Stueben D, Berner Z, Ramanivosoa B, Randriamanantenasoa A (2002) Age and paleoenvironment of the Maastrichtian-Paleocene of the Mahajanga Basin, Madagascar: a multidisciplinary approach. Mar Micropaleontol 47:17–70

Adatte T, Keller G, Stinnesbeck W (2002) Late Cretaceous to early Paleocene climate and sea-level fluctuations: the Tunisian record. Palaeogeogr Palaeoclimatol Palaeoecol 178:165–196

Ali JR, Aitchison JC (2008) Gondwana to Asia: plate tectonics, paleogeography and the biological connectivity of the Indian sub-continent from the Middle Jurassic through latest Eocene (166–35 Ma). Earth Sci Rev 88:145–166

Arthur MA, Dean WE, Schlanger SO (1985) Variations in the global carbon cycle during the Cretaceous related to climate,

volcanism, and changes in atmospheric CO_2. Geophys Monogr Ser 32:504–529
Bains S, Corfield RM, Norris RD (1999) Mechanisms of climate weathering at the end of the Paleocene. Science 285:724–727
Bandara AS, Weerasinghe DA, Ratnayake AS (2020) Determination of the regional and residual gravity anomalies to reconstruct basin structures of the Cauvery Basin. J Geol Soc Sri Lanka 21:21–31
Bender MM (1971) Variations in the $^{13}C/^{12}C$ ratios of plants in relation to the pathway of photosynthetic carbon dioxide fixation. Phytochemistry 10:1239–1244
Berner RA (1982) Burial of organic carbon and pyrite sulfur in the modern ocean: its geochemical and environmental significance. Am J Sci 282:451–473
Berner RA (1984) Sedimentary pyrite formation: an update. Geochim Cosmochim Acta 48:605–615
Berner RA, Lasaga AC, Garrels RM (1983) The carbonate-silicate geochemical cycle and its effect on atmospheric carbon dioxide over the past 100 million years. Am J Sci 283:641–883
Bingham EM, McClymont EL, Väliranta M, Mauquoy D, Roberts Z, Chambers FM, Pancost RD, Evershed RP (2010) Conservative composition of *n*-alkane biomarkers in *Sphagnum* species: implications for palaeoclimate reconstruction in ombrotrophic peat bogs. Org Geochem 41:214–220
Bose S, Das A, Samantaray S, Banerjee S, Gupta S (2020) Late tectonic reorientation of lineaments and fabrics in the northern Eastern Ghats Province, India: evaluating the role of the Mahanadi Shear Zone. J Asian Earth Sci 201:104071
Boss SK, Wilkinson BH (1991) Planktogenic/eustatic control on cratonic/oceanic carbonate accumulation. J Geol 99:497–513
Caldeira K, Rampino MR (1993) Aftermath of the end-Cretaceous mass extinction: possible biogeochemical stabilization of the carbon cycle and climate. Paleoceanography 8:515–525
Calvès G, Schwab AM, Huuse M, Clift PD, Giana C, Jolley D, Tabrez AR, Inam A (2011) J Geophys Res 116:B01101. https://doi.org/10.1029/2010JB000862
Castañeda IS, Werne JP, Johnson TC, Filley TR (2009) Late Quaternary vegetation history of southeast Africa: the molecular isotopic record from Lake Malawi. Palaeogeogr Palaeoclimatol Palaeoecol 275:100–112
Chakraborty PP, Tandon SK, Saha S (2019) Development of Phanerozoic sedimentary basins of India. J Asian Earth Sci 184:103991
Chatterjee S, Goswami A, Scotese CR (2013) The longest voyage: tectonic, magmatic, and paleoclimatic evolution of the Indian plate during its northward flight from Gondwana to Asia. Gondwana Res 23:238–267
Chikaraishi Y, Naraoka H (2005) $\delta^{13}C$ and δD identification of sources of lipid biomarkers in sediments of Lake Haruna (Japan). Geochim Cosmochim Acta 69:3285–3297
Chung SL, Lo CH, Lee TY, Zhang Y, Xie Y, Li X, Wang KL, Wang PL (1998) Diachronous uplift of the Tibetan plateau starting 40 Myr ago. Nature 394:769–773
Clift PD (2020) Asian monsoon dynamics and sediment transport in SE Asia. J Asian Earth Sci 195:104352.
Cooray PG (1984) An introduction to the geology of Sri Lanka. 2nd revised edition, Ceylon National Museum Publication, Colombo, pp. 135–169.
D'Hondt S, Donaghay P, Zachos JC, Luttenberg D, Lindinger M (1998) Organic carbon fluxes and ecological recovery from the Cretaceous-Tertiary mass extinction. Science 282:276–279
Davies TA, Kidd RB, Ramsay STS (1995) A time-slice approach to the history of Cenozoic sedimentation in the Indian Ocean. Sed Geol 96:157–179
Desa M, Ramana MV, Ramprasad T (2006) Seafloor spreading magnetic anomalies south off Sri Lanka. Mar Geol 229:227–240
Dettman DL, Kohn MJ, Quade J, Ryerson FJ, Ojha TP, Hamidullah S (2001) Seasonal stable isotope evidence for a strong Asian monsoon throughout the past 10.7 m.y. Geology 29:31–34
Dissanayake CB, Chandrajith R (1999) Sri Lanka-Madagascar Gondwana linkage: evidence for a Pan-African mineral belt. J Geol 107:223–235
Dypvik H, Riber L, Burca F, Rüther D, Jargvoll D, Nagy J, Jochmann M (2011) The Paleocene-Eocene thermal maximum (PETM) in Svalbard – clay mineral and geochemical signals. Palaeogeogr Palaeoclimatol Palaeoecol 302:156–169
Ficken KJ, Li B, Swain DL, Eglinton G (2000) An *n*-alkane proxy for the sediment input of submerged/ floating freshwater aquatic macrophytes. Org Geochem 31:745–749
France-Lanord C, Derry LA (1997) Organic carbon burial forcing of the carbon cycle from Himalayan erosion. Nature 390:65–67
Gaillardet J, Galy A (2008) Himalaya-carbon sink or source? Science 320:1727–1728
Gaina C, Müller RD, Brown B, Ishihara T, Ivanov S (2007) Breakup and early spreading between India and Antarctica. Geophys J Int 170:151–169
Gertsch B, Keller G, Adatte T, Garg R, Prasad V, Berner Z, Fleitmann D (2011) Environmental effects of Deccan volcanism across the Cretaceous-Tertiary transition in Meghalaya, India. Earth Planet Sci Lett 310:272–285
Gombos AM, Powell WG, Norton IO (1995) The tectonic evolution of western India and its impact on hydrocarbon occurrences: an overview. Sed Geol 96:119–129
Gong C, Hollander DJ (1997) Differential contribution of bacteria to sedimentary organic matter in oxic and anoxic environments, Santa Monica Basin, California. Org Geochem 26:545–563
Gupta AK, Singh RK, Joseph S, Thomas E (2004) Indian Ocean high-productivity event (10–8 Ma): linked to global cooling or to the initiation of the Indian monsoons? Geology 32:753–756
Gupta S, Kumar K (2019) Precursors of the Paleocene-Eocene Thermal Maximum (PETM) in the Subathu Group, NW sub-Himalaya, India. J Asian Earth Sci 169:21–46
Harris N (2006) The elevation history of the Tibetan Plateau and its implications for the Asian monsoon. Palaeogeogr Palaeoclimatol Palaeoecol 241:4–15
Hickey LJ, Doyle JA (1977) Early Cretaceous fossil evidence for angiosperm evolution. Bot Rev 43:3–104
Hong SK, Yi S, Shinn YJ (2020) Middle Albian climate fluctuation recorded in the carbon isotope composition of terrestrial plant matter. J Asian Earth Sci 196:104363
Huber BT, Watkins DK (1992) Biogeography of Campanian-Maastrichtian calcareous plankton in the region of the Southern Ocean: paleogeographic and paleoclimatic implications. The Antarctic Paleoenvironment: A Perspective on Global Change 56:31–60
Ibach LEJ (1982) Relationship between sedimentation rate and total organic carbon content in ancient marine sediments. Am Asso Petrol Geol Bull 66:170–188
Kaiho K, Kajiwara Y, Tazaki K, Ueshima M, Takeda N, Kawahata H, Arinobu T, Ishiwatari R, Hirai A, Lamolda MA (1999) Oceanic primary productivity and dissolved oxygen levels at the Cretaceous/Tertiary boundary: their decrease, subsequent warming, and recovery. Paleoceanography 14:511–524
Kapawar MR, Mamilla V (2020) Paleomagnetism and rock magnetism of early Cretaceous Rajmahal basalts, NE India: implications for paleogeography of the Indian subcontinent and migration of the Kerguelen hotspot. J Asian Earth Sci 201:104517
Keller G (2003) Biotic effects of impacts and volcanism. Earth Planet Sci Lett 215:249–264
Keller G (2004) Low-diversity, late Maastrichtian and early Danian planktic foraminiferal assemblages of the eastern Tethys. J Foramin Res 34:49–73

Keller G (2005) Biotic effects of late Maastrichtian mantle plume volcanism: implications for impacts and mass extinctions. Lithos 79:317–341

Keller G, Adatte T, Gardin S, Bartolini A, Bajpai S (2008) Main Deccan volcanism phase ends near the K-T boundary: evidence from the Krishna-Godavari Basin, SE India. Earth Planet Sci Lett 268:293–311

Keller G, Punekar J, Mateo P (2015) Upheavals during the Late Maastrichtian: volcanism, climate and faunal events preceding the end-Cretaceous mass extinction. Palaeogeogr Palaeoclimatol Palaeoecol 441:137–151

Kent DV, Muttoni G (2008) Equatorial convergence of India and early Cenozoic climate trends. Proc Natl Acad Sci 105:16065–16070

Kularathna EKCW, Pitawala HMTGA, Senaratne A, Ratnayake AS (2020) Play distribution and the hydrocarbon potential of the Mannar Basin, Sri Lanka. Journal of Petroleum Exploration and Production Technology 10:2225–2243

Lamb AL, Wilson GP, Leng MJ (2006) A review of coastal palaeoclimate and relative sea-level reconstructions using $\delta^{13}C$ and C/N ratios in organic material. Earth Sci Rev 75:29–57

Lasitha S, Twinkle D, Kurian PJ, Harikrishnan PR (2019) Geophysical evidence for marine prolongation of the Palghat-Cauvery shear system into the offshore Cauvery basin, Eastern continental margin of India. J Asian Earth Sci 184:103981

Le Fort P (1975) Himalayas: the collided range, present knowledge of the continental arc. Am J Sci 275:1–44

Lees JA (2002) Calcareous nannofossil biogeography illustrates palaeoclimate change in the Late Cretaceous Indian Ocean. Cretac Res 23:537–634

Li T, Huang Z, Yin Y, Gou H, Zhang P (2020) Sedimentology and geochemistry of Cretaceous source rocks from the Tiancao Sag, Yin'e Basin, North China: implications for the enrichment mechanism of organic matters in small lacustrine rift basins. J Asian Earth Sci 204:104575

Licht A, Cappelle MV, Abels HA, Ladant JB, Alexandre JT, Lanord CF, Donnadieu Y, Vandenberghe J, Rigaudier T, Lécuyer C, Terry D Jr, Adriaens R, Boura A, Guo Z, Soe AN, Quade J, Nivet GD, Jaeger JJ (2014) Asian monsoons in a late Eocene greenhouse world. Nature 513:501–506

Lokho K, Aitchison JC, Whiso K, Lhoupenyi D, Zhou R, Raju DSN (2020) Eocene foraminifers of the Naga Hills of Manipur, Indo-Myanmar Range (IMR): implications on age and basin evolution. J Asian Earth Sci 191:104259

Lourens LJ, Sluijs A, Kroon D, Zachos JC, Thomas E, Röhl U, Bowles J, Raffi I (2005) Astronomical pacing of late Palaeocene to early Eocene global warming events. Nature 435:1083–1086

Lu N, Wang YD, Popa ME, Xie XP, Li LQ, Xi SN, Deng CT (2019) Sedimentological and paleoecological aspects of the Norian-Rhaetian transition (Late Triassic) in the Xuanhan area of the Sichuan Basin, Southwest China. Palaeoworld 28:334–345

McKenzie D, Sclater JG (1971) The evolution of the Indian Ocean since the late Cretaceous. Geophysics Journal 25:437–528

Métivier F, Gaudemer Y, Tapponnier P, Klein M (1999) Mass accumulation rates in Asia during the Cenozoic. Geophys J Int 137:280–318

Meyers PA (2003) Applications of organic geochemistry to paleolimnological reconstructions: a summary of examples from the Laurentian Great Lakes. Org Geochem 34:261–289

Meyers PA, Ishiwatari R (1993) Lacustrine organic geochemistry–an overview of indicators of organic matter sources and diagenesis in lake sediments. Org Geochem 20:867–900

Molnar P, Tapponnier P (1975) Cenozoic tectonics of Asia: effects of a continental collision. Science 189:419–426

Müller PJ (1977) C/N ratios in Pacific deep-sea sediments: effect of inorganic ammonium and organic nitrogen compounds sorbed by clays. Geochim Cosmochim Acta 41:765–776

Nair N, Pandey DK (2018) Cenozoic sedimentation in the Mumbai Offshore Basin: implications for tectonic evolution of the western continental margin of India. J Asian Earth Sci 152:132–144

Norton IO, Sclater JG (1979) A model for the evolution of the Indian Ocean and the breakup of Gondwanaland. J Geophys Res 84:6803–6830

O'Keefe JD, Ahrens TJ (1989) Impact production of CO_2 by the Cretaceous/Tertiary extinction bolide and the resultant heating of the Earth. Nature 338:247–249

Pälike H, Norris RD, Herrle JO, Wilson PA, Coxall HK, Lear CH, Shackleton NJ, Tripati AK, Wade BS (2006) The heartbeat of the Oligocene climate system. Science 314:1894–1898

Pancost RD, Bass M, Geel BV, Damste JSS (2002) Biomarkers as proxies for plant inputs to peats: an example from a sub-boreal ombrotrophic bog. Org Geochem 33:675–690

Parmar V, Jamwal SS, Prasad GV, Palden L (2020) An Oligo-Miocene cricetid rodent from the Indus Group, NW Himalaya: constraints on the age of initiation of continental sedimentation in the India-Asia collision zone. J Asian Earth Sci 190:104190

Pearson PN, Foster GL, Wade BS (2009) Atmospheric carbon dioxide through the Eocene-Oligocene climate transition. Nature 461:1110–1113

Pearson PN, Palmer MR (2000) Atmospheric carbon dioxide concentrations over the past 60 million years. Nature 406:695–699

Qin SX, Li YX, Li XH, Xu B, Luo H (2019) Paleomagnetic results of Cretaceous cherts from Zhongba, southern Tibet: new constraints on the India-Asia collision. J Asian Earth Sci 173:42–53

Quade J, Cerling TE, Bowman JR (1989) Development of Asian monsoon revealed by marked ecological shift during the latest Miocene in northern Pakistan. Nature 342:163–166

Ramana MV, Ramprasad T, Desa M (2001) Seafloor spreading magnetic anomalies in the Enderby Basin, East Antarctica. Earth Planet Sci Lett 191:241–255

Rao GN (2001) Sedimentation, stratigraphy and petroleum potential of Krishna-Godavari Basin, East Coast of India. Am Asso Petrol Geol Bull 85:1623–1643

Rao GS, Singh A (2020) Crustal architecture and isostatic compensation of the Comorin Ridge, central Indian Ocean: implications for the breakup of east Gondwana. J Asian Earth Sci 199:104463

Ratnayake AS, Kularathne CW, Sampei Y (2018) Assessment of hydrocarbon generation potential and thermal maturity of the offshore Mannar Basin, Sri Lanka. J Pet Explor Prod Technol 8:641–654

Ratnayake AS, Sampei Y (2015) Characterization of organic matter and depositional environment of the Jurassic small sedimentary basins exposed in the northwest onshore area of Sri Lanka. Researches in Organic Geochemistry 31:15–28

Ratnayake AS, Sampei Y (2019) Organic geochemical evaluation of contamination tracers on deepwater rock cutting from the Mannar Basin, Sri Lanka. J Pet Explor Prod Technol 9:989–996

Ratnayake AS, Sampei Y, Kularathne CW (2014) Stratigraphic responses to major depositional events from the Late Cretaceous to Miocene in the Mannar Basin, Sri Lanka. Journal of Geological Society of Sri Lanka 16:5–18

Ratnayake AS, Sampei Y, Ratnayake NP, Roser BP (2017) Middle to late Holocene environmental changes in the depositional system of the tropical brackish Bolgoda Lake, coastal southwest Sri Lanka. Palaeogeogr Palaeoclimatol Palaeoecol 465:122–137

Raymo ME, Ruddiman WF (1992) Tectonic forcing of late Cenozoic climate. Nature 359:117–122

Rea DK, Dehn J, Driscoll NW, Farrell JW, Janecek TR, Owen RM, Pospichal JJ, Resiwati P (1990) Paleoceanography of the Eastern Indian-Ocean from ODP Leg-121 drilling on Broken Ridge. Geol Soc Am Bull 102:679–690

Ridgwell A, Zeebe RE (2005) The role of the global carbonate cycle in the regulation and evolution of the Earth system. Earth Planet Sci Lett 234:299–315

Rotstein Y, Munschy M, Bernard A (2001) The Kerguelen Province revisited: additional constraints on the early development of the Southeast Indian Ocean. Mar Geophys Res 22:81–100

Sampei Y, Matsumoto E (2001) C/N ratios in a sediment core from Nakaumi Lagoon. southwest Japan. Geochem J 35:189–205

Sampei Y, Matsumoto E, Kamei T, Tokuoka T (1997a) Sulfur and organic carbon relationship in sediments from coastal brackish lakes in the Shimane Peninsula District, southwest, Japan. Geochem J 31:245–262

Sampei Y, Matsumoto E, Tokuoka T, Inoue D (1997b) Changes in accumulation rate of organic carbon during the last 8000 years in sediments of Nakaumi Lagoon, Japan. Mar Chem 58:39–50

Scotese, C.R., Illich, H., Zumberge, J., Brown, S., Moore, T., 2011. The GANDOLPH Project: Year Four Report: Paleogeographic and Paleoclimatic Controls on Hydrocarbon Source Rock Deposition, A Report on the Methods Employed, the Results of the Paleoclimate Simulations (FOAM), and Oils/Source Rock Compilation for the Oligocene (30 Ma), Cretaceous/Tertiary (70 Ma), Permian/Triassic (250 Ma), Silurian/ Devonian (400 Ma), and Cambrian/Ordovician (480 Ma), Conclusions at the End of Year Four, April 2011. GeoMark Research Ltd., Houston, Texas. 219 pp

Sigurdsson H, D'Hondt S, Carey S (1992) The impact of the Cretaceous/Tertiary bolide on evaporite terrane and generation of major sulfuric acid aerosol. Earth Planet Sci Lett 109:543–559

Sreejith KM, Krishna KS, Bansal AR (2008) Structure and isostatic compensation of the Comorin Ridge, north central Indian Ocean. Geophys J Int 175:729–741

Storey M, Mahoney JJ, Saunders AD, Duncan RA, Kelley SP, Coffin MF (1995) Timing of hot spot-related volcanism and the breakup of Madagascar and India. Science 267:852–855

Subrahmanyam C, Chand S (2006) Evolution of the passive continental margins of India – a geophysical appraisal. Gondwana Res 10:167–178

Tantawy AAA, Keller G, Pardo A (2009) Late Maastrichtian volcanism in the Indian Ocean: effects on calcareous nannofossils and planktic foraminifera. Palaeogeogr Palaeoclimatol Palaeoecol 284:63–87

Teng X, Fang X, Kaufman AJ, Liu C, Wang J, Zan J, Piatak NM (2019) Sedimentological and mineralogical records from drill core SKD1 in the Jianghan Basin, Central China, and their implications for late Cretaceous–early Eocene climate change. J Asian Earth Sci 182:103936

Tripati AK, Roberts CD, Eagle RA (2009) Coupling of CO_2 and ice sheet stability over major climate transitions of the last 20 million years. Science 326:1394–1397

Valdés J, Sifeddine A, Lallier-Verges E, Ortlieb L (2004) Petrographic and geochemical study of organic matter in surficial laminated sediments from an upwelling system (Mejillones del Sur Bay, Northern Chile). Org Geochem 35:881–894

Volk T (1989) Sensitivity of climate and atmospheric CO_2 to deep-ocean and shallow-ocean carbonate burial. Nature 337:637–640

Yang H, Huang Y, Ma C, Zhang Z, Wang C (2020) Recognition of Milankovitch cycles in XRF core-scanning records of the Late Cretaceous Nenjiang Formation from the Songliao Basin (northeastern China) and their paleoclimate implications. J Asian Earth Sci 194:104183

Zachos J, Pagani M, Sloan L, Thomas E, Billups K (2001) Trends, rhythms, and aberrations in global climate 65 Ma to present. Science 292:686–693

Zachos JC, Arthur MA, Dean WE (1989) Geochemical evidence for suppression of pelagic marine productivity at the Cretaceous/Tertiary boundary. Nature 337:61–64

Zachos JC, Dickens GR, Zeebe RE (2008) Early Cenozoic perspective on greenhouse warming and carbon-cycle dynamics. Nature 451:279–283

Zachos JC, Röhl U, Schellenberg SA, Sluijs A, Hodell DA, Kelly DC, Thomas E, Nicolo M, Raffi I, Lourens LJ, McCarren H, Kroon D (2005) Rapid acidification of the ocean during the Paleocene-Eocene thermal maximum. Science 308:1611–1615

Zhisheng A, Kutzbach JE, Prell WL, Porter SC (2001) Evolution of Asian monsoons and phased uplift of the Himalaya-Tibetan plateau since Late Miocene times. Nature 411:62–66

Zhou W, Xie S, Meyers PA, Zheng Y (2005) Reconstruction of late glacial and Holocene climate evolution in southern China from geolipids and pollen in the Dingnan peat sequence. Org Geochem 36:1272–1284